

DESIGN OF DUAL BAND MONOPOLE ANTENNA FOR BLUETOOTH AND ULTRA WIDE BAND WITH TRIPLE NOTCH USING ELECTROMAGNETIC BANDGAP STRUCTURE

TAPAN MANDAL¹, PRASANTA MANDAL², PRATIK MONDAL³, LAKHINDAR MURMU⁴

Keywords: Bluetooth; Ultra-wideband, Electromagnetic band gap structure, WiMAX, WLAN, X-band.

This paper focuses on the applications of dual band antenna for Bluetooth (2.4 – 2.484 GHz) and ultra-wideband (3.1 – 10.6 GHz) with triple notch band. A spanner shape with a rectangular strip monopole and the partial rectangular ground plane is used as the desired dual band antenna. The electromagnetic bandgap EBG structures are placed near the feed line to obtain notch frequencies at 3.5 GHz, 5.5 GHz, and 7.5 GHz. The detailed parametric study of the antenna is presented and discussed. The input impedance and current distributions are used for the effects of EBG and narrow strips. Test results of the fabricated design show a good similarity with simulated outcomes, validating design principles. The designed antenna exhibits nearly omnidirectional radiation patterns, stable gain, appreciable efficiency, linear phase, and constant group delay over the desired bands. Hence the proposed antenna is expected to be suitable for both Bluetooth and UWB applications.

1. INTRODUCTION

Nowadays, dozens of wireless communication systems and portable devices rapidly change our lifestyles. All communication systems often require an antenna which is an essential component. Due to limited space and easy integration to the circuit board, a multiband antenna [1] is the demand in the modern era for various uses within a module. ultra-wideband (UWB) technology is a key solution due to many attractive features and its advantages [2]. Then UWB antennas have been widely investigated by industry and academia since 2002. Many techniques are used to design UWB antennae with impedance bandwidth (BW), stable radiation pattern, constant group delay, and linear phase [3–9]. In addition to UWB, the Bluetooth (IEEE 802.15; 2.4–2.484 GHz) band is also quite popular in the industrial, scientific, and medical fields (ISM 2.4 GHz) due to its elegant advantages [7, 8] and numerous applications in the wireless devices. The modern wireless communication system requires an integration of UWB and Bluetooth systems that link devices as diverse as fixed and portable appliances, PCs, and entertainment equipment. However, the Bluetooth band is not considered in the design [3–6, 9–22]. This issue is taken care of in this paper.

Some existing standard narrow bands such as WiMAX (IEEE 802.16: 3.3–3.7 GHz), WLAN (IEEE 802.11a: 5.15 – 5.825 GHz), and downlink of X-band (7.25 – 7.75 GHz) satellite communication system operate in the UWB spectrum. These existing bands degrade the reliable performance of UWB system due to interference. To avoid such interferences from the UWB device, a UWB with band rejection characteristics is desirable. The band rejection performance is achieved by several methods, for example, inserting slots in different shapes on the feed line [9], radiator [7, 9–11], ground plane [6, 9], and parasitic strips near the antenna [11]. The shortcoming of the parasitic element is that it requires large space on the antenna and strong coupling

between the notching element [13]. The mushroom structure has been studied widely to produce a notched band [12–22], gain enhancement [14, 15], BW enhancement [16], good isolation [14, 17], and surface wave reduction [18]. A comparative study of the designed antenna with existing literature is presented in Table 1. From Table 1, it is evident that most papers have a single (WLAN band only) or dual notch band (WiMAX and WLAN band) in the UWB frequency range without integrating the Bluetooth frequency band. Moreover, the reported antennas may have a complex structure or be larger, or the notch frequency is not sufficiently tuned. The microstrip fed UWB with single notch band characteristics and Bluetooth band have been proposed in [7]. This configuration is complex and cannot be easily integrated into the MMIC. This issue is also conceived here.

Table 1
Comparison of proposed design with existing papers

Ref.	Size (mm ²)	Type of EBG	ϵ_r/h (mm)	No. of EBG	Operating band (GHz)	No. N. B. (center freq. of NB in GHz)
[13]	38×40	ELV	4.4 / 1.0	1	3.1–10.6	2 (3.6 / 5.5)
[18]	39×35	CMT	3.38 / 0.8	4	3.1–10.6	1 (5.5)
[19]	38×40	ELV	4.5 / 1.0	1	3.1 - -	1 (5.59)
[20]	32×52	ELV	4.4 / 1.6	3	2.81–14.32	2 (3.5 / 5.5)
[21]	42×50	CMT	4.4 / 1.6	4	–	2 (3.4 / 5.4)
[22]	42×50	CMT	4.4 / 1.6	2	–	2 (3.49/5.43)
Prop	32×50	ELV	4.4 / 1.6	4	2.36–2.50 2.94 – >12	3 (3.5/5.5/7.5)

In this paper, a microstrip fed trident shaped dual-band printed antenna for Bluetooth and UWB with triple notch characteristics has been proposed. It has a combination of

¹Department of Information Technology, ²Dept. of Computer Science and Engineering, ^{1,2}Govt. College of Engineering and Textile Technology, Serampore, Hooghly, India, PIN – 712201, ¹tapanmandal20@rediffmail.com; ²prasanta.anshin@gmail.com

³Department of Electronics and Communication Engineering, Gayatri Vidya Parishad College of Engineering (Autonomous), Visakhapatnam- 530 048, India, pratik665@gmail.com

⁴Department of Electronics and Communication Engineering, Dr. SPM International Institute of Information Technology, Naya Raipur, Chhattisgarh, India, lakhindar.kgec25@gmail.com

geometric shapes: a spanner patch, rectangular strip, and rectangular ground. Spanner-shaped and rectangular strip monopole elements provide UWB and Bluetooth bands, respectively. The notch bands (NB) are achieved by implanting a mushroom-like EBG structure in the vicinity of the feed line. By adjusting the mushroom parameters, the desired notch frequency, as well as notch BW, can be controlled sufficiently. All the parametric study is done through the IE3D™ simulator. The characteristics of the proposed antenna are studied in terms of frequency and time domains. Surface current distributions are built at the same time for analysis and explanation of band-notch properties. It has an operating range for Bluetooth and UWB in the frequency regions of 2.36 GHz to 2.50 GHz and 2.94 GHz to >12.00 GHz, respectively, for $|S_{11}| \leq -10$ dB with an excellent rejection band of WiMAX, WLAN and X-band to prevent the signals. An EBG has better control than the prevalent techniques.

2. ANTENNA DESIGN CONSIDERATION

2.1. UWB ANTENNA

Figure 1 depicts the topology of the proposed antenna. In Fig. 1, the spanner shape radiator is created by incorporating a rectangular slot (with $L_s \times W_s$) within the hexagonal patch radiator. The idea of carving out a slot from the patch conceives by examining the current distribution. Each configuration is designed on a FR 4 substrate ($32 \times 52 \times 1.59$ mm³) with permittivity, $\epsilon_r = 4.4$, loss tangent, $\tan\delta = 0.02$. All the configurations have (i) radiator patch, (ii) microstrip line, and (iii) ground plane. A 50Ω microstrip line is connected to the patch for excitation. The patch and microstrip line is designed on one side of a substrate, whereas the ground plane (in a rectangular shape) is taken on the opposite side of the same radiator. A rectangular slot under the feed line can adjust the electromagnetic coupling effects between the radiating patch and the ground plane to improve impedance BW. In addition, rectangular steps within the radiating patch are used to adjust the impedance BW over the UWB frequency band.

A rectangular shape strip is inserted in the slot section of the spanner monopole antenna to achieve the desired Bluetooth band. The length (L_B) of the narrow strip is about a quarter-wave long at the central Bluetooth band frequency (f_B).

2.2. UWB ANTENNA WITH BAND NOTCH

To avoid the WiMAX band from the UWB range, a pair of EBG cells is integrated into the vicinity of the microstrip line. By employing a pair of mushroom cells, a strong rejection signal is achieved. The EBG cells are sited symmetrically concerning the microstrip line. The notch frequency is related to the dimension of the mushroom. Though, the rough size of the mushroom patch can be estimated as

$$p = \frac{300}{2f_{notch} \sqrt{\frac{(\epsilon_r + 1)}{2}}}, \quad (1)$$

where p is the perimeter ($p = 2(\text{length} + \text{breadth})$) of the mushroom patch in mm.

For WiMAX band, the center notch frequency $f_{notch} = 3.5$ GHz the perimeter of the rectangular mushroom is calculated as 26.13 mm. The length and width of the rectangular mushroom cell can be easily determined

through an EM solver, IE3D.

In addition to this, to avoid the WLAN and X-band (downlink of satellite communication) from the UWB span, another two mushroom structures of different sizes are placed near the microstrip line. All optimized geometric parameters are listed in Table 2.

2.3. MICROSTRIP LINE BASED EBG MODEL

The EBG structure consists of a metallic plate which is connected to ground by a shortening pin named via. The plate

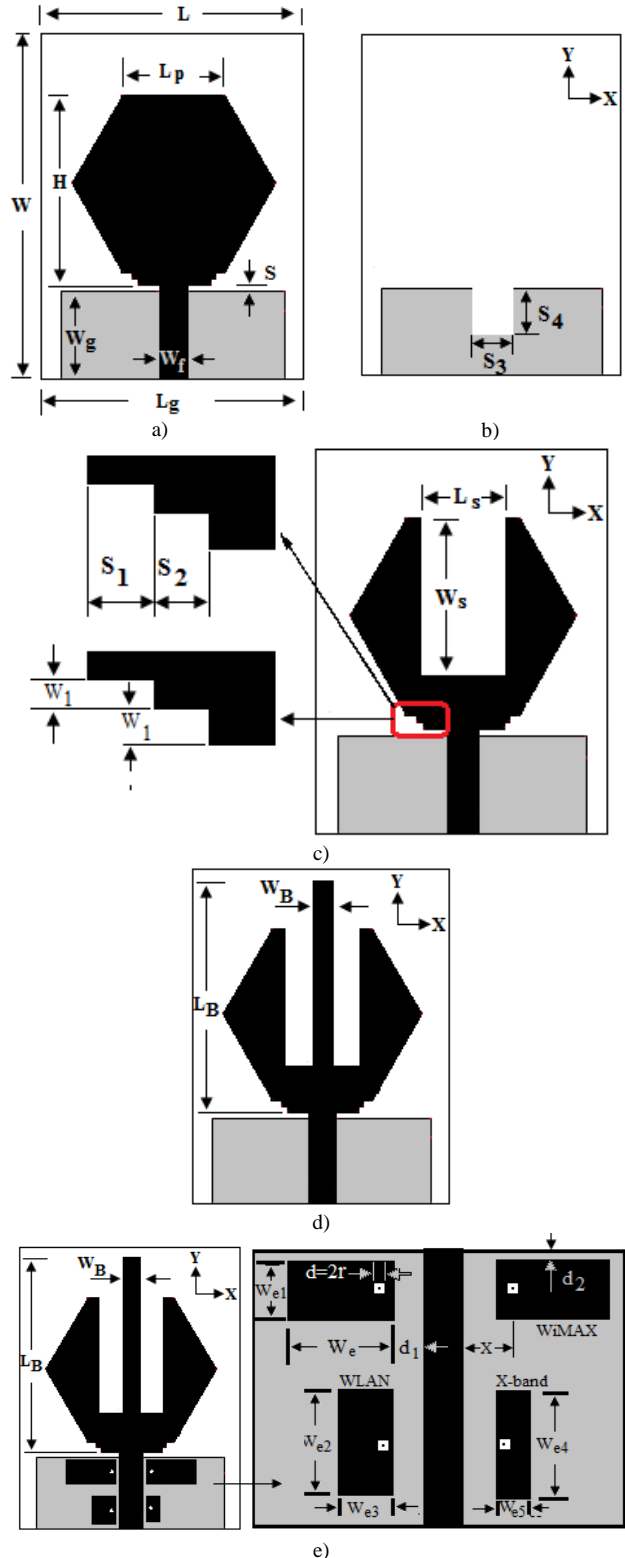


Fig. 1 – Geometry of monopole antenna: a) hexagon; b) ground plane; c) spanner; d) spanner and rectangular strip; e) proposed.

behaves as a capacitance whereas via provides the inductance at the stop band (SB). The resonant frequency (f_r) of the EBG unit can be determined as equation (2).

$$f_r = \frac{1}{2\pi\sqrt{L(C_0 + C_1)}}. \quad (2)$$

The inductance of metallic via (L) is caused by the flow of current through the shorting via, and the voltage gradient between the EBG patch and ground plane provides capacitance (C_0). The coupling gap capacitance (C_1) is generated between the feed line and EBG cell.

Table 2
Antenna dimensions (in mm)

Parameter	L	W	L_p	H	L_g	W_g	S
Dimension	32	50	10.5	19.38	28	13.5	0.8
Parameter	W_f	S_3	S_4	S_1	S_2	W_1	L_s
Dimension	2.8	3.1	2	1	0.5	0.68	8
Parameter	W_s	L_B	W_B	W_e	W_{e1}	d_1	$d = 2r$
Dimension	12.38	28	2	7.8	4.9	0.28	0.3
Parameter	X	d_2	W_{e2}	W_{e3}	W_{e4}	W_{e5}	
Dimension	0.55	0.22	5.7	3.7	5.4	0.19	

3. RESULTS AND DISCUSSION

3.1. PARAMETRIC STUDY AND EXPLANATIONS

To identify the resonance modes of Fig. 1a and Fig. 1c, the input impedance and $|S_{11}|$ are plotted respectively in Fig. 2 and Fig. 3. From Fig. 2 and Fig. 3, it is observed that the resistance is close to 50Ω while the reactance is not far from 0Ω . It indicates that a good impedance matching is obtained for a wide frequency range, leading to a UWB characteristic. The Bluetooth band is independently created by inserting a rectangular strip within the slot section of the spanner monopole *i.e.*, Fig. 1d. Figure 4 illustrates the simulated $|S_{11}|$ characteristics for various values of length (L_B) of the strip. It is observed from Fig. 4 that the notch band moves leftwards with a higher peak as the length of strip is increased. The strip length has excellent impact on shifting the frequency. The central resonating frequency and impedance BW of this band can be easily controlled by the geometric parameters.

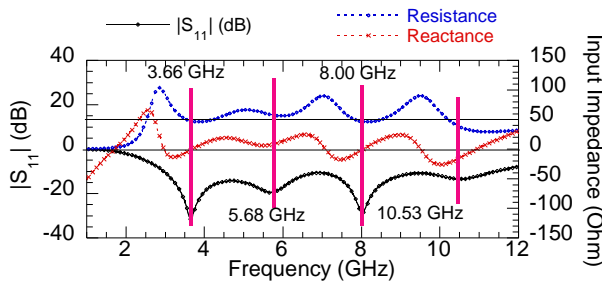


Fig. 2 – Curve of $|S_{11}|$ and input impedance for Fig. 1a.

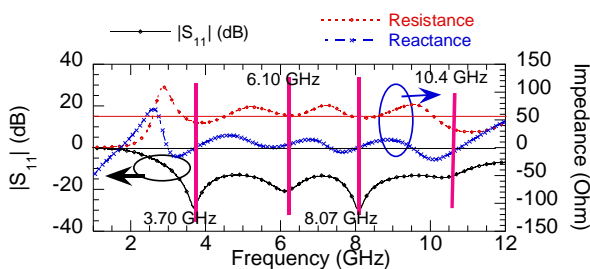


Fig. 3 – Curve of $|S_{11}|$ and input impedance for Fig. 1c.

Therefore Fig. 1d provides dual-band operation (Bluetooth and UWB) due to two different resonant elements. Figures 5 and 6 represent the $|S_{11}|$ curve for different arm length (W_e and W_{e1}) of the EBG. From the characteristics, it is observed that as the arm length of EBG increases, the notch band shift towards the left side of the plot. This is due to the rise of EBG patch area, which is responsible for increased capacitance. Thus, the patch arm offers sufficient freedom for selecting the desired notch

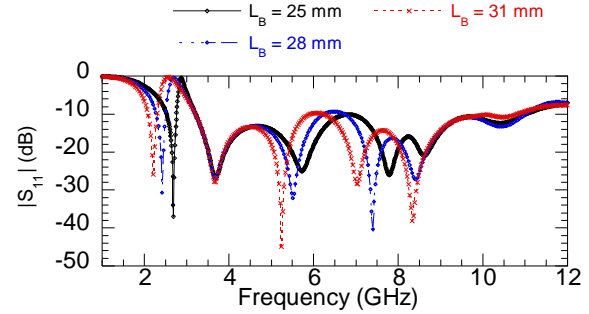


Fig. 4 – Curve of $|S_{11}|$ versus frequency for different L_B .

within the mushroom. Figure 7 depicts the band-rejection feature varying the position of via within the mushroom. As shown in Fig. 7, the position of via at the edge has much sharper rejection properties than at the center. An edge-located mushroom generates a higher $|S_{11}|$ value at the notch frequency with narrow notch BW due to better coupling. Figure 8 shows the variation of $|S_{11}|$ for different values of d_1 , representing the gap between the mushroom cell and feed line. From the response, it is regarded that the lower values of d_1 , yield broader and better band rejection properties in the notched band. Also, the decreasing gap between the two structures increases the coupling capacitance, moving the notch-band to lower frequencies with a strong rejection signal.

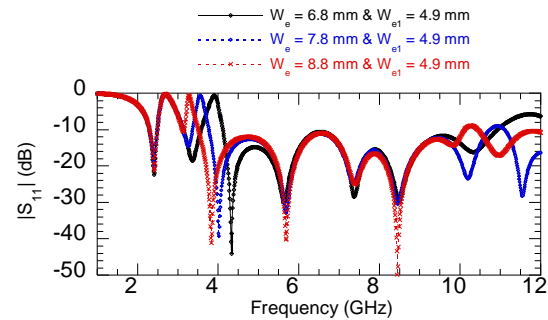


Fig. 5 – Curve of $|S_{11}|$ versus freq. with different W_e for WiMAX notch.

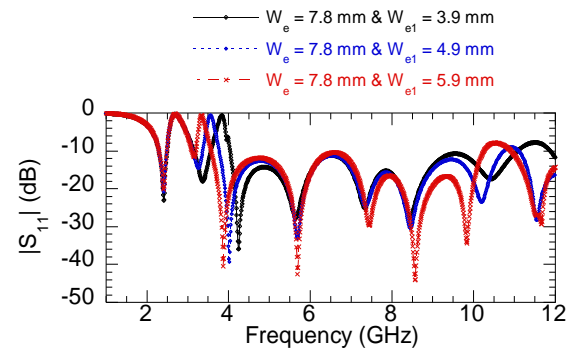


Fig. 6 – Curve of $|S_{11}|$ versus freq. with different W_{e1} for WiMAX notch.

Figure 9 illustrates the variation of $|S_{11}|$ for different values via diameter, d . As shown, the diameter of via (d) decreases,

and the center frequency of the notch band moves to the lower frequency range with some decrease in BW due to the inductance related to via increases. The via diameter has ample scope to control the notch frequency. Furthermore, to avoid the WLAN and X-band downlink in UWB region two more EBG has been used in the prototype antenna, as shown in Fig. 1. For comparison, the magnitude of $|S_{11}|$ curve of different designed configurations is given in Fig. 10. From the curves, the antenna without EBG structure works as a UWB antenna. In contrast, each EBG structure stops a band in the proposed configuration. The Bluetooth band is created due to the narrow strip, while the spanner is responsible for the UWB band.

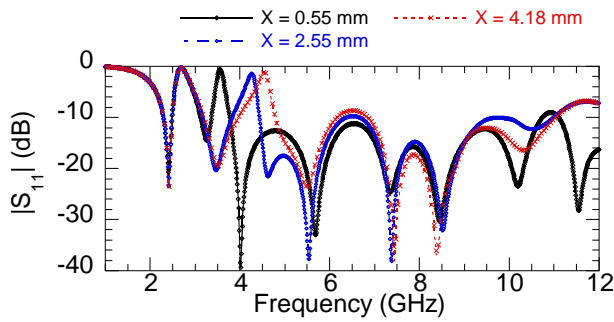


Fig. 7 – Curve of $|S_{11}|$ versus freq. with the variation of via position X .

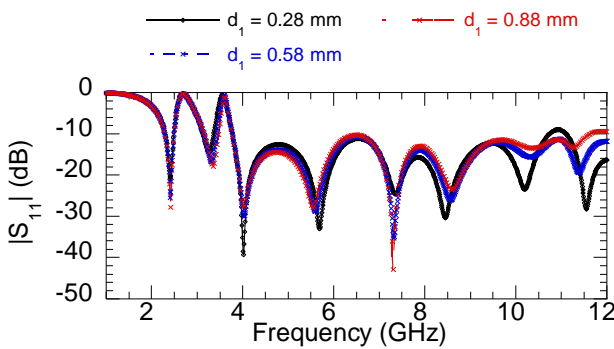


Fig. 8 – Curve of $|S_{11}|$ versus freq. with the variation of gap d_1 .

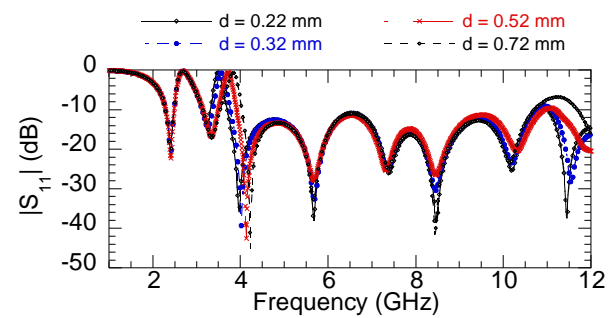


Fig. 9 - Curve of $|S_{11}|$ versus freq. with the variation of via diameter d .

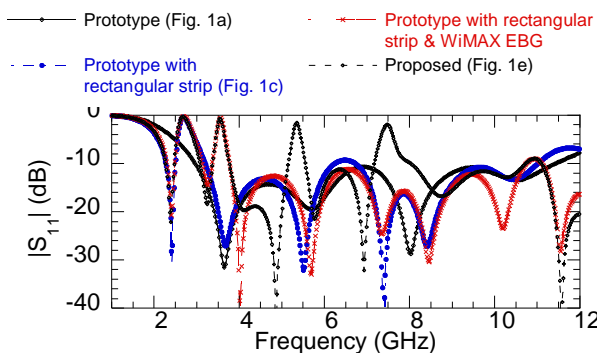


Fig. 10 – Comparative study of the $|S_{11}|$ versus freq. characteristics.

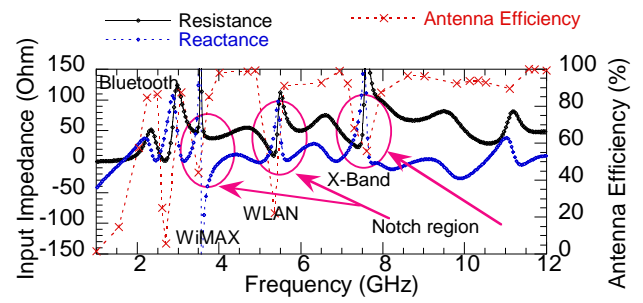


Fig. 11 – Input impedance and efficiency of proposed antenna.

The proposed structure has good impedance matching (Fig. 11) over the whole operating range, where sharp changes at 3.5 GHz, 5.5 GHz, and 7.5 GHz which results in a steep rise of $|S_{11}|$. This drastic change of impedance indicates that most of the power feed into the antenna is reflected, which leads to a decrease in the antenna efficiency. It remains above 90 % throughout the operating band.

3.2. CURRENT DISTRIBUTION FOR ANALYSIS

Numerical vector current distributions of Fig. 1 (e) are shown in Fig. 12, which is used to investigate the effect of the pass band and notch band. The surface current at 2.45 GHz and 3.24 GHz are mainly concentrated at the narrow strip and patch, while a negligible number of current flows to the mushroom (Figs. 12 a, b) cells.

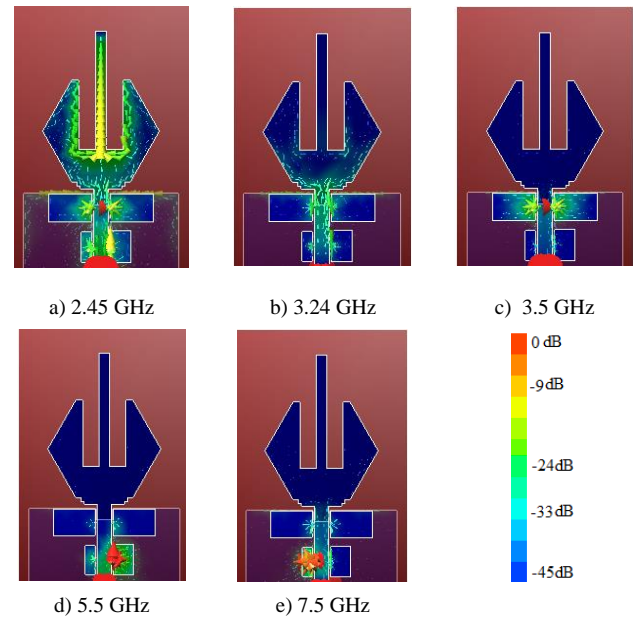


Fig 12 – Numerical current distribution of Fig. 1e.

This phenomenon indicates the presence of mushrooms within the structure has a minor effect on the pass band. As shown in Fig. 12c, d, e, most of the current is concentrated on the mushroom, whereas a little amount of current appears on the patch. It justifies that the EBG operates as a resonator, and the equivalent LC circuit behaves as a short-circuit resulting in surface current reflected in the input port. It indicates that the radiation is blocked, and the notched bands are created in the UWB range.

4. FABRICATION AND MEASUREMENT RESULT

A snapshot of the fabricated antennas is shown in Fig. 13. The impedance BW of the antenna is measured with an Agilent make (Model: N5230A) vector network

analyzer. To verify the validity of the design idea, impedance BW is measured. The simulation and tested curves of the prototype and proposed antenna are shown respectively in Fig. 14 and 15. From Fig. 14, it is observed that both the response covers the whole UWB range, and the tested results comply with the simulated one. Thus, it may be considered a good UWB antenna. For comparison, the magnitude of S_{11} ($|S_{11}| \leq -10$ dB) characteristics of the proposed antenna are shown in Fig. 15, and the results are given in Table 3. The proposed antenna successfully rejects three bands from the UWB frequency span.

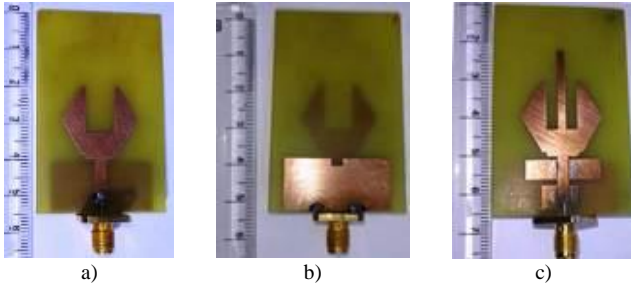


Fig. 13 – Photo of antenna: a) prototype (top); b) prototype (ground); c) proposed (top).

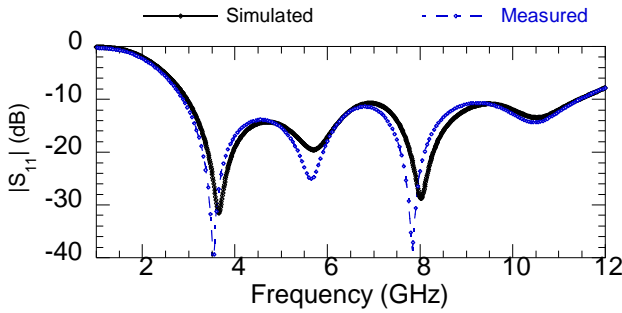


Fig. 14 – $|S_{11}|$ versus frequency of Fig. 13a.

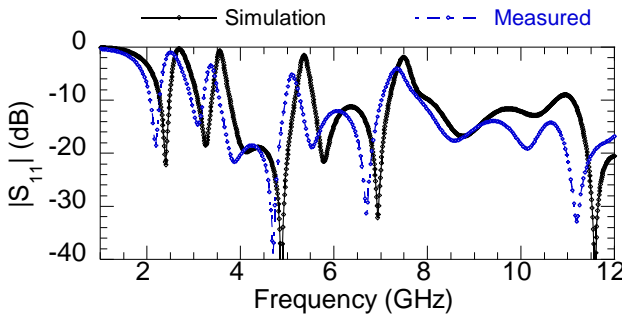


Fig. 15 – $|S_{11}|$ versus frequency 13c.

Table 3

Comparison of $|S_{11}|$ (all frequencies in GHz; f_L – lower frequency and f_H – higher frequency).

Band	Bluetooth		UWB		WiMAX		WLAN		X-Band		
	f_L	f_H	f_L	f_H	f_L	f_H	f_L	f_H	f_L	f_H	
Proto (Simu)	—	—	2.97	11.43	—	—	—	—	—	—	
Proto (Meas)	—	—	2.88	11.44	—	—	—	—	—	—	
Propo (Simu)	2.40	2.54	3.09	10.7	3	3.38	3.78	5.16	5.70	7.28	8.03
Propo (Meas)	2.36	2.50	2.94	>12.	0	3.3	3.7	5.09	5.6	7.15	7.8

A minor difference is observed due to the following reasons: (i) fabrication error; (ii) wide flange of SM; (iii) via dimension, and (iv) solder roughness. Figure 16 presents the radiation patterns of Fig. 13a and 13c. The patterns for both antennas have good similarities. Thus, the introductions of EBGs have a minor effect on the patterns. The antenna has a dipole-like radiation pattern and a good omnidirectional radiation pattern in the E-plane and H-plane, respectively. The radiation patterns are reasonably stable over both Bluetooth and UWB bands. Thus, it may consider a good dual band antenna. From Fig. 16, the patterns for both antennas have good similarities. Therefore, the introductions of EBGs have a minor effect on the patterns.

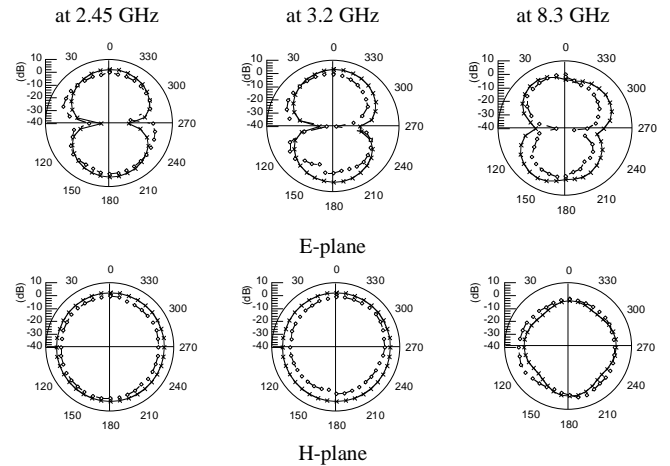


Fig. 16 – Co-polar measured radiation patterns (—×— prototype, —◇— proposed).

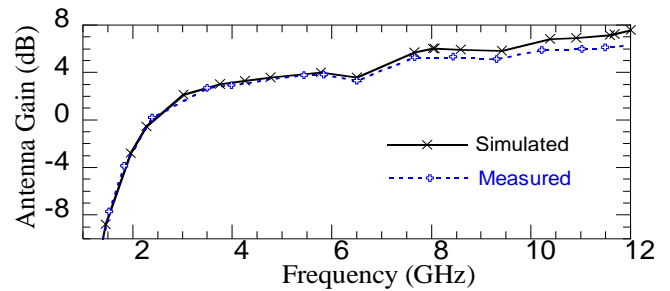


Fig. 17 – Antenna gain of prototype antenna.

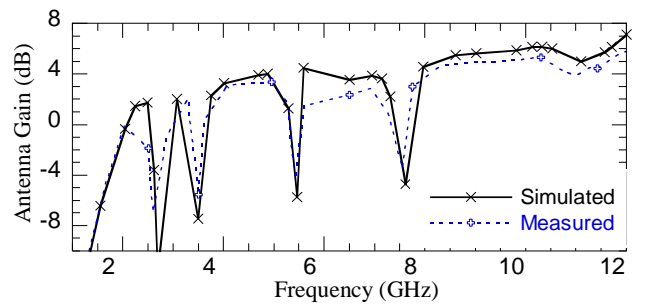


Fig. 18 – Antenna gain of the proposed antenna.

The gain comparisons of the prototype and proposed antenna are plotted respectively in Fig. 17 and Fig. 18. The tested result agrees well with the simulated one, as is evident from the plots. From Fig. 18, the designed antenna gain varies from 2.3 – 5.2 dB, where the gain drastically decreases at the notch region within the UWB range. Thus, the antenna has a stable flat gain over the operating frequency range.

5. TIME DOMAIN STUDY

The time domain analysis has a significant aspect for Bluetooth and UWB antenna. A very small distortion is desirable at the transmitting and receiving end for the efficient performance of the antenna. The group delay of the proposed antenna is depicted in Fig. 19. The performances of group delay remain almost constant (within 2 ns) throughout the entire operating range except for the notch bands. The phase of S_{21} (Fig. 20) is quite linear within the desired bands, excluding the notch bands in face-to-face mode. It confirms that the antenna has a good time-domain characteristic.

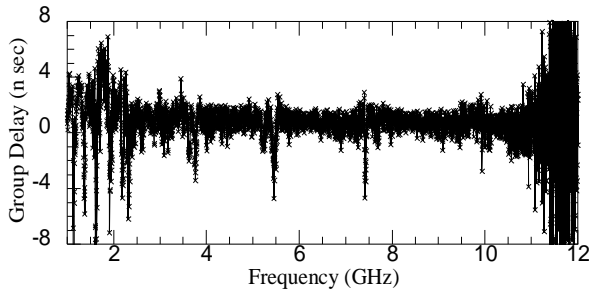


Fig. 19 – Measured group delay of the proposed antenna.

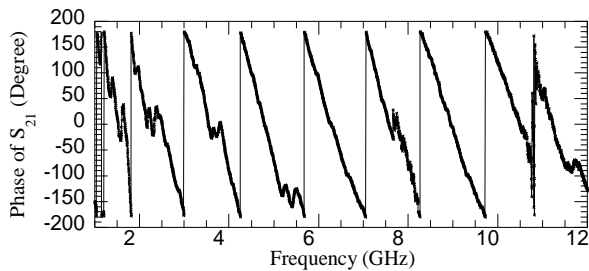


Fig. 20 – Measured phase of the proposed antenna.

6. CONCLUSION

In this paper, a microstrip-fed dual band antenna for Bluetooth and UWB with triple stop bands has been designed, investigated, and proposed. The Bluetooth band is achieved by integrating a strip in the slot section of the spanner shape, whereas UWB is obtained due to the spanner structure. The antenna can operate through the impedance BW spreading from 2.36 GHz to 2.50 GHz and 2.94 GHz to >12 GHz. The desired stop bands (WiMAX: 3.3 – 3.7 GHz, WLAN: 5.09 – 5.6 GHz, and X-band: 7.15 – 7.80 GHz) are realized by mushroom structures within the UWB frequency span. A detailed parametric study is carried out to investigate the effects on the pass band and stop band. The existence of the mushroom structure does not perturb the behaviour of the radiation pattern. The gain response of the proposed antenna is the same as the prototype antenna. Gain varies from 2.3 – 5.2 dB within the operating band of the designed configuration. In addition, the designed antenna has quite satisfactory time domain performance, which makes it a good candidate for Bluetooth and UWB systems.

Received on 18 February 2021

REFERENCES

1. M. Samsuzzaman, M.T. Islam, M.J. Singh, *Ceramic material based multiband patch antenna for satellite applications*, Rev. Roum. Sci. Techn. – Électrotechn. et Énerg., **59**, 1, pp. 77–85, (2014).
2. Federal Communications Commission, *Revision of Part 15 of the Commission's Rule Regarding Ultra-Wideband Transmission system FCC 02-48*, First Report and Order, 2002.
3. J. Liu, S. Zhong, K. P. Esselle, *A printed elliptical monopole antenna with modified feeding structure for bandwidth enhancement*, IEEE Transactions on Antennas and Propagation, **59**, 2, pp. 667–670 (2011).
4. J. Liang, L. Guo, C.C. Chiau, X. Chen, C.G. Parini, *Study of CPW-fed circular disc monopole antenna*, IEE Microwaves, Antennas and Propagation, **152**, 6, pp. 520–526 (2005).
5. X.J. Liao, H.C. Yang, N. Han, Y. Li, *Aperture UWB antenna with triple band-notched characteristics*, Electronics Letters, **47**, 2 (2011).
6. D. Abed, S. Redadaa, H. Kimouche, *Printed ultra-wideband stepped circular slot antenna with different tuning stubs*, Journal of Electromagnetic Waves and Applications, **27**, 7, pp. 846–855 (2013).
7. S.K. Mishra, R. Gupta, A. Vaidya, J. Mukherjee, *Printed fork-shaped dual-band monopole antenna for Bluetooth and UWB applications with 5.5 GHz WLAN band-notched characteristics*, Progress in Electromagnetics Research C, **22**, pp. 195–210 (2011).
8. T. Mandal, S. Das, *Design of a microstrip fed printed monopole antenna for Bluetooth and UWB applications with WLAN notch band characteristics*, International Journal of RF and Microwave Computer-Aided Engineering, **25**, 1, pp. 66–71 (2015).
9. M. Chakraborty, S. Pal, N. Chatteraj, *Quad notch UWB antenna using a combination of slots and split-ring resonator*, Int. Journal of RF and Computer Aided Engineering, **30**, 3, pp. 1–10 (2019).
10. A. Sohail et al. *Dual notch band uwb antenna with improved notch characteristics*, Microwave and Optical Technology Letter, **60**, 4, pp. 925–930 (2018).
11. D. Sarkar, K.V. Srivastava, K. Saurav, *A compact microstrip-fed triple band-notched UWB monopole antenna*, IEEE Antennas and Wireless Propagation Letters, **13**, pp. 396–399 (2014).
12. S. Peddakrishna, T. Khan, *Design of UWB monopole antenna with dual notched band characteristics by using p-shaped slot and EBG resonator*, AEU Int. Journal Electron Communication, **96**, pp. 107–112 (2018).
13. H. Liu, Z. Xie, *Design of UWB monopole antenna with dual notched bands using one modified electromagnetic band gap structure*, The Scientific World Journal, **2013**, 917965 (2013).
14. H.H. Xie, Y.C. Jiao, L.N. Chen, F.S. Zhang, *Omnidirectional horizontally polarized antenna with EBG cavity for gain enhancement*, Progress In Electromagnetics Research Letters, **15**, pp. 79–87 (2010).
15. A. Ghosh et al., *Gain enhancement of triple-band patch antenna using triple-band artificial magnetic conducto*, IET Microwave Antennas Propagation, **12**, 8, pp. 1400–1406 (2018).
16. A. Pirhadi, M. Hakkak, F. Keshmiri, *Using electromagnetic band gap superstrate to enhance the bandwidth of probe-fed microstrip antenna*, Progress in Electromagnetics Research, **61**, pp. 215–230 (2006).
17. R. Mäkinen, V. Pynttari, J. Heikkinen, M. Kivikoski, *Improvement of antenna isolation in hand-held devices using miniaturized electromagnetic band gap structures*, Microwave and Optical Technology Letters, **49**, 10, pp. 2508–2513 (2007).
18. M. Yazdi, N. Komjani, *Design of a band-notched UWB monopole antenna by means of an EBG structure*, IEEE Antenna and Wireless Propagation Letters, **10**, pp. 170–173 (2011).
19. L. Peng, C.L. Ruan, *UWB band-notched monopole antenna design using electromagnetic-bandgap structures*, IEEE Transactions on Microwave Theory and Technique, **59**, 4, pp. 1074–1081 (2011).
20. T. Mandal, S. Das, *Design of a CPW-fed UWB printed antenna with dual notch band using mushroom structure*, Int. J. Microw. Wireless Tech., **9**, 2, pp. 327–334 (2017).
21. N. Jaglan, B.K. Kanaujia, S.D. Gupta, S. Srivastava, *Design and development of an efficient EBG structures based band notched UWB circular monopole antenna*, Wireless Personal Communications, **96**, 4, pp. 5757–5783 (2017).
22. N. Jaglan, B.K. Kanaujia, S.D. Gupta, S. Srivastava, *Band notched UWB circular monopole antenna with inductance enhanced modified mushroom EBG structures*, Wireless Personal Communications, **24**, 2, pp. 383–393 (2018).